PAPER

Active Contours Driven by Local Rayleigh Distribution Fitting Energy for Ultrasound Image Segmentation

Hui BI[†a)], ***Student Member***, **Yibo JIANG**[††b)], **Hui LI**[††], **Xuan SHA**[†††], ***and*** **Yi WANG**[††††], ***Nonmembers***

SUMMARY The ultrasound image segmentation is a crucial task in many clinical applications. However, the ultrasound image is difficult to segment due to image inhomogeneity caused by the ultrasound imaging technique. In this paper, to deal with image inhomogeneity with considering ultrasound image properties the Local Rayleigh Distribution Fitting (LRDF) energy term is introduced into the traditional level set method newly. While the curve evolution equation is derived for energy minimization, and self-driven uterus contour is achieved on the ultrasound images. The experimental segmentation results on synthetic images and in-vivo ultrasound images present that the proposed approach is effective and accurate, with the Dice Score Coefficient (DSC) of 0.95 ± 0.02.

key words: *ultrasound image segmentation, Rayleigh mixture model, level set, neighbor information*

1. Introduction

The uterus fibroid is commonly occurring benign tumors that annoy females and segmentation of uterus fibroid is a crucial target in clinical applications. However, precise segmentation is a challenge to achieve since intensity inhomogeneity [1]. Intensity inhomogeneity occurs in medical images due to technical limitations or artifacts introduced by the organ being imaged [2]–[4]. The active contour models have been used as image segmentation methods widely [5]–[7]. It can be categorized into two classes as edge-based and region-based models. *Chan* and *Vese* proposed several classic region-based models likes CV model and Piece-Smooth (PS) model [8]. The region-based models perform better than edge-based for weak object boundaries images, attribute to non-utilizing of the image gradient. Furthermore, it is less sensitive to the location of initial contours. To deal with intensity inhomogeneity of image, authors proposed some energy fitting term into active contours method [9], [10]. *Li* proposed a Local Binary Fitting (LBF) energy in a region-based model for more accuracy and efficient segmentation for MRI images [11]. While *Wang* proposed a local Gaussian Distribution Fitting (LGDF) energy to distinguish regions with same intensity mean and different intensity variances [12]. *Yu* also proposed an efficient level set model for medical image segmentation [13]. However, these methods are not suitable for the medical ultrasound images segmentation, because the whole ultrasound image information is mainly composed of speckle patterns that be specific to each tissue as well as the micro in-homogeneities.

Some researchers have utilized statistics distribution to characterize the observed tissue, and demonstrated that the statistics of one tissue follow the Rayleigh distribution for the ultrasound images [14], [15]. In this paper, we proposed a method incorporated the local information into a region-based active contour model for uterus ultrasound image segmentation. The local intensity information, which is proposed as the Local Rayleigh Distribution Fitting (LRDF) energy, is introduced into region-based active contour model. The local energy is integrated over the whole image domain by double integral function. The curve evolution constrained by minimizing the energy function is used for variance computation and guide the contour motion. The remainder of this paper is organized as follows. Section 2 introduces the proposed LRDF model. Section 3 presents and discusses experiments on a set of synthetic and in-vivo ultrasound images. Finally, we conclude the paper in Sect. 4.

2. Local Rayleigh Distribution Fitting

In this section, an implicit active contour model based on local information is proposed for ultrasound image segmentation. Considering ultrasound image properties the Rayleigh distribution rather than Gaussian Distribution is utilized to demonstrate local information. The Local Rayleigh Distribution Fitting (LRDF) energy term is defined and the LRDF energy is incorporated into a level set method. With minimizating energy the curve evolution processes to achieve self-driven tissues contour in ultrasound images. The model is described in detail as follows.

2.1 Local Rayleigh Distribution Fitting Energy Term

The Fig. 1 is gray histogram analysis for ultrasound image. Because of the speckle its intensity distribution is revealed to be the Rayleigh distributions. As Fig. 2 shown, the Ω and $x \in \Omega$ denote image domain and this image consists of two regions: Ω_1 and Ω_2. Each point in the image, a neigh-

Manuscript received October 18, 2017.
Manuscript revised December 20, 2017.
Manuscript publicized February 8, 2018.

†The author is with Changzhou University, Changzhou, Jiangsu, China.
††The authors are with the Changzhou Institute of Technology, Changzhou, Jiangsu, China.
†††The author is with the Southeast University Chengxian College, Nanjing, Jiangsu, China.
††††The author is with the Chongqing Medical University, Chongqing, China.
a) E-mail: bihui@seu.edu.cn
b) E-mail: jiangyb@czust.edu.cn

DOI: 10.1587/transinf.2017EDP7344

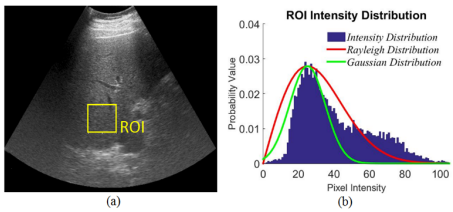

Fig. 1 Histogram of ultrasound image: (a) ROI of original ultrasound image; (b) Histogram of ROI.

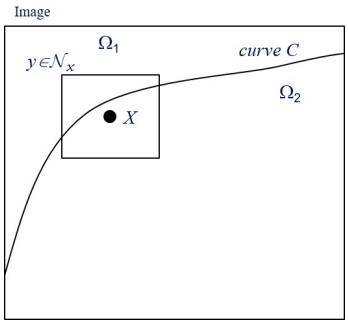

Fig. 2 Graphical representation of $\Omega_i \cap \mathcal{N}_x$. The outer square denotes the whole image and the inner square denotes the neighbor region $\mathcal{N}_x$ of point x. According to representation of the Ω_1 and Ω_2, $\mathcal{N}_x$ is divided into sub-regions $\Omega_1 \cap \mathcal{N}_x$ and $\Omega_2 \cap \mathcal{N}_x$.

borhood region is defined as $\mathcal{N}_x \triangleq \{y : |x-y| \le \rho\}$. The ρ denotes the radius of the region. Let $\left\{\Omega_{i=1}^{N}\right\}$ be a set of disjoint regions of the whole image, such that $\Omega = \bigcup_{i=1}^{N} \Omega_i$ and $\Omega_i \cap \Omega_j = \varnothing$, $\forall i \ne j$, where the N refers to the number of regions. The region $\mathcal{N}_x \triangleq \{y : |x-y| \le \rho\}$ is divided into two sub-regions as $\Omega_1 \cap \mathcal{N}_x$ and $\Omega_2 \cap \mathcal{N}_x$.

Based on maximum a posteriori probability (MAP), the segmentation of this neighborhood $\mathcal{N}_x \triangleq \{y : |x-y| \le \rho\}$ is reconsidered as follows. Let $p(y \in \Omega_i \cap \mathcal{N}_x | I(y))$ be the posteriori probability of the sub-regions $\Omega_i \cap \mathcal{N}_x$, by given the neighborhood gray values $I(y)$. As *Wang* mentioned in [12], $p(I(y)|y \in \Omega_i \cap \mathcal{N}_x)$ is modeled by a Gaussian distribution. While in our approach the probability densities $p(I(y)|y \in \Omega_i \cap \mathcal{N}_x)$ is modeled by a Rayleigh distribution for uterus ultrasound images. The variance of the local Rayleigh distribution is spatially varying parameters.

$$p(I(y)|y \in \Omega_i \cap \mathcal{N}_x) = \frac{I(y)}{\sigma_i^2(x)} \exp(-\frac{I(y)^2}{2\sigma_i^2(x)}) \tag{1}$$

where $\sigma_i(x)$ denotes the standard deviations in the region $\Omega_i \cap \mathcal{N}_x$. We introduce an energy term based on Rayleigh distributions and converted it to the logarithm form for simplified calculation.

$$\begin{aligned} E_x^{LRDF} &= -\sum_{i=1}^{N} \int_{\Omega_i \cap \mathcal{N}_x} \log p(I(y)|\Omega_i \cap \mathcal{N}_x) dy \\ &= -\sum_{i=1}^{N} \int_{\Omega_i \cap \mathcal{N}_x} [\log I(y) + \log \sigma_i^2(x) - \frac{I(y)^2}{2\sigma_i^2(x)}] dy \end{aligned} \tag{2}$$

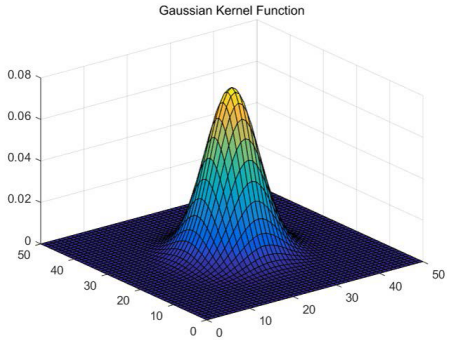

Fig. 3 Gaussian Kernel function.

$$\begin{aligned} E_x^{LRDF} = -\sum_{i=1}^{N} \int_{\Omega_i \cap \mathcal{N}_x} & \omega(y-x)[\log I(y) + \log \sigma_i^2(x) \\ & - \frac{I(y)^2}{2\sigma_i^2(x)}] dy \end{aligned} \tag{3}$$

Here a weighting function $\omega(\|\bullet\|)$ is introduced by the truncated Gaussian function also, to improve Eq. (2) into Eq. (3). The shape of Gaussian kernel function on the assumption that the center $x = 25$ and $\sigma_g^2 = 25$ is showed in Fig. 3.

2.2 Level Set Formulation

It is assumed that the uterus ultrasound image domain can be partitioned into two regions as uterine fibroid and the other. These two regions Ω_1 and Ω_2 represented the regions outside and inside the zero level set of ϕ : $\Omega_1 = \{\phi > 0\}$ and $\Omega_2 = \{\phi < 0\}$, respectively. While the energy function of the image defined by Eq. (4) could be expressed in terms of ϕ and σ_i^2 as follows.

$$\begin{aligned} & E_x^{LRDF}(\phi, \sigma_1^2(x), \sigma_2^2(x)) = \\ & \quad -\int \omega(y-x) \log p(I(y)|y \in \Omega_1 \cap \mathcal{N}_x) H(\phi) dy \\ & \quad -\int \omega(y-x) \log p(I(y)|y \in \Omega_2 \cap \mathcal{N}_x) [1 - H(\phi)] dy \end{aligned} \tag{4}$$

where $H(\phi)$ is Heaviside fuction, $H(\phi) = 1$ if $\phi > 0$, while $H(\phi) = 0$ if $\phi < 0$. Thus, the energy of the whole image can be expressed as

$$E^{LRDF} = \int_{\Omega} E_x^{LRDF}(\phi, \sigma_1^2(x), \sigma_2^2(x))\, dx \tag{5}$$

To avoid re-initialization in level set evolution, a penalty term have been proposed by *Li* [11]:

$$\mathcal{P}(\phi) = \int \frac{1}{2}(|\nabla \phi\,(x)| - 1)^2 dx \tag{6}$$

Meanwhile, the curve length penalty term also needs to be considered as

$$\mathcal{L}(\phi) = \int |\nabla H(\phi(x))| dx \tag{7}$$

Therefore, the entire energy function can be expressed as

$$\mathcal{F}(\phi, \sigma_1^2(x), \sigma_2^2(x)) = E^{LRDF}(\phi, \sigma_1^2(x), \sigma_2^2(x)) + \nu\mathcal{L}(\phi) + \mu\mathcal{P}(\phi) \tag{8}$$

where both $\nu > 0$ and $\mu > 0$ are weighting constants. In practice, a smoothing function H_ε is adopted to approximate the Heaviside function H and the derivative of H_ε is demonstrated by

$$\delta_\varepsilon(x) = H_\varepsilon'(x) = \frac{1}{\pi}\frac{\varepsilon}{\varepsilon^2 + x^2} \tag{9}$$

The energy function $\mathcal{F}_\varepsilon(\phi, \sigma_1^2(x), \sigma_2^2(x))$ in Eq. (8) is approximated by

$$\mathcal{F}_\varepsilon(\phi, \sigma_1^2(x), \sigma_2^2(x)) = E_\varepsilon^{LRDF}(\phi, \sigma_1^2(x), \sigma_2^2(x)) + \upsilon\mathcal{L}_\varepsilon(\phi) + \mu\mathcal{P}(\phi) \tag{10}$$

2.3 Gradient Descent Flow

To minimize the energy function described in Eq. (10), the gradient descent flow is adopted to obtain the parameters σ_1^2 and σ_2^2. For a fix ϕ the σ_1^2 satisfies the Euler-Lagrange equations as follows [11].

$$\frac{\partial\mathcal{F}_\varepsilon(\phi, \sigma_1^2(x), \sigma_2^2(x))}{\partial\sigma_1^2(x)} = 0 \tag{11}$$

From Eq. (11), we obtain

$$\sigma_1^2(x) = \frac{1}{2}\frac{\int \omega(y-x)I(y)^2M_1(\phi)dy}{\int \omega(y-x)M_1(\phi)dy} \tag{12}$$

where $M_1(\phi) = H(\phi)$, $M_2(\phi) = 1 - H(\phi)$. While $w(y-x)$ denotes Gaussian function window. Its value will be close to 1 if the y is close to x. Similarly, parameter σ_2^2 is obtained by the following equation.

$$\frac{\partial\mathcal{F}_\varepsilon(\phi, \sigma_1^2(x), \sigma_2^2(x))}{\partial\sigma_2^2(x)} = 0 \tag{13}$$

$$\sigma_2^2(x) = \frac{1}{2}\frac{\int \omega(y-x)I(y)^2M_2(\phi)dy}{\int \omega(y-x)M_2(\phi)dy} \tag{14}$$

It is noticeable that the formulas of $\sigma_2^2(x)$ is similar to Ref. [12]. The reason is that the Rayleigh density formula is similar to the Gaussian density formula with the mean $u_i(x) = 0$. The energy function $\mathcal{F}_\varepsilon(\phi, \sigma_1^2(x), \sigma_2^2(x))$ with the ϕ is minimized through solving the gradient descent flow equation as follows.

$$\frac{\partial\phi}{\partial t} = -\delta_\varepsilon(e_1 - e_2) + \upsilon\delta_\varepsilon(\phi)div\left(\frac{\nabla\phi}{|\nabla\phi|}\right) + \mu\left(\nabla^2\phi - \mathrm{div}\left(\frac{\nabla\phi}{|\nabla\phi|}\right)\right) \tag{15}$$

where

$$e_1(x) = \int_\Omega \omega(y-x)\left(\log\sigma_1^2(x) + \frac{I^2(y)}{2\sigma_1^2(x)} - \log I(y)\right)dx \tag{16}$$

$$e_2(x) = \int_\Omega \omega(y-x)\left(\log\sigma_2^2(x) + \frac{I^2(y)}{2\sigma_2^2(x)} - \log I(y)\right)dx \tag{17}$$

3. The Synthetic and In-Vivo Medical Images Experiments

In this section, the experiments on synthetic and in-vivo medical images are showed and discussed in detail. Firstly, the experiments on synthetic images with anatomical realism carry out as shown in Fig. 4. The Fig. 4 (a) is composed of an elliptically-shaped region within a background region. The simulated method predicts the appearance and the properties of a B-Scan ultrasound image from a probe model with a C2-5 circular ultrasound scanning 3.5 MHz. The size of the synthetic image is 1352×1149. The initial contour of the ultrasound image is shown in Fig. 4 (b). After 60 iterations the final segmentation result is obtained by our approach as shown in Fig. 4 (c). It is indicated that the contour of the ellipse is achieved through the curve evolution after 60 iterations by the proposed method.

In the experiments on in-vivo images, our proposed method is compared with two methds such as conventional level set method and LBP method proposed by *Li* [11] on uterine ultrasound images segmentation. As shown in Fig. 5, there are eight images from different patients numbered from #1 to #8. The red, yellow and green lines denote LRDF, LBF and conventional level set results, respectively. It is obvious that the LRDF results present more accurate uterine contours, attribute to that the ultrasound image properties are taken into account and a local distribution fitting as an energy term into the level set formulation. Furthermore, a quantitative accuracy analyses between our self-driven method and specialist manual segmentation are sum-

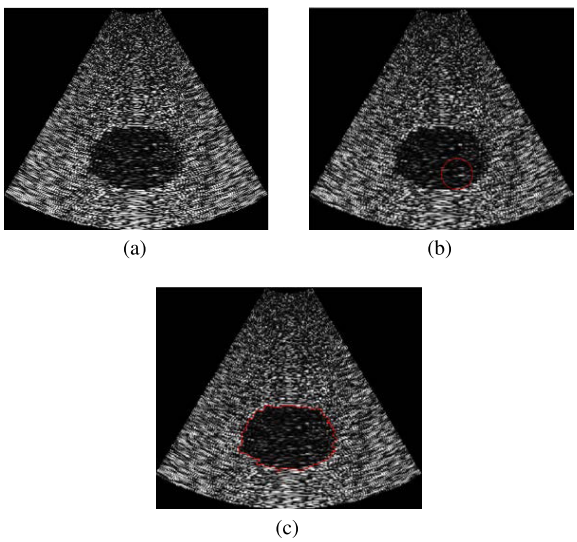

Fig. 4 Results of LRDF for the synthetic image. (a) Synthetic image. (b) The initial contour of the level set. (c) Object contour.

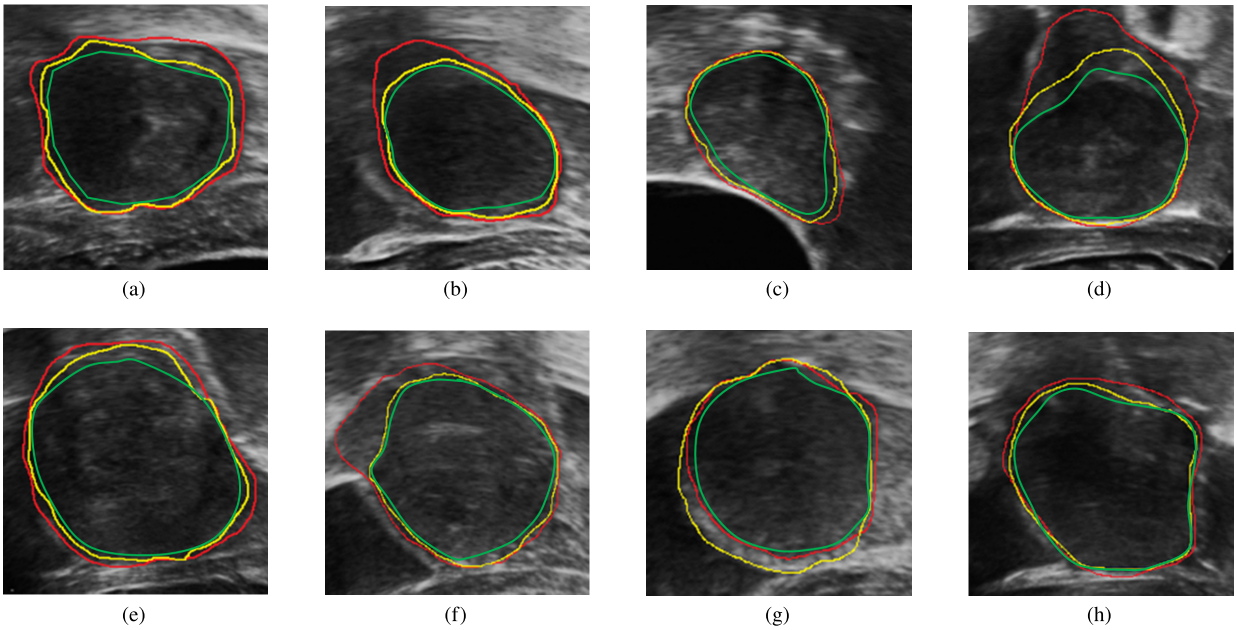

Fig. 5 The segmentation results for uterus images. The red, yellow and green lines denote LRDF, LBF and conventional level set results, respectively.

Table 1 The accuracy summary of the Levet set, LBF and LRDF.

	Level set	LBF	LRDG
#1	0.78	0.90	0.95
#2	0.76	0.87	0.96
#3	0.72	0.88	0.89
#4	0.82	0.86	0.96
#5	0.79	0.89	0.90
#6	0.76	0.82	0.89
#7	0.76	0.79	0.91
#8	0.82	0.85	0.88
#9	0.82	0.89	0.91

marized based on the Dice Similarity Coefficient (DSC). The DSC is an evaluating standards defined in Ref. [16] as

$$DSC(S_S, S_R) = \frac{2Area(S_S \cap S_R)}{Area(S_S) + Area(S_R)} \tag{18}$$

where S_S and S_R denote segmentation results and ground truth, respectively. The value of DSC is closer to 1, the segmentation result is better. As shown in Table 1 it is indicated that the LRDF is the most accurate quantificationally.

4. Conclusion

In this paper, for ultrasound image segmentation we proposed a novel method of active contours driven by local Rayleigh distribution fitting energy. To deal with image inhomogeneity the LRDF is introduced as an additive energy term to level set method. Through our approach the uteruscan can be self-driven segmented in the medical image. Moreover, the segmentation experiments on synthetic and in-vivo images demonstrated that the proposed method achieve accuracy segmentation results than the state of the art methods, with the DSC can reach 0.95 ± 0.02.

Acknowledgments

This work is supported by Key Program of Changzhou Institute of Technology (Grant No. YN1634) and Natural Science Foundation of the Jiangsu Higher Education Institutions of China (17KJB416001).

References

[1] J.A. Noble and D. Boukerroui, "Ultrasound image segmentation: a survey," IEEE Trans. Med. Imag., vol.25, no.8, pp.987–1010, 2006.
[2] T. Joel and R. Sivakumar, "Despeckling of ultrasound medical images: A survey," Journal of Image & Graphics, pp.161–165, 2013.
[3] W. Zhao, H. Lu, and D. Wang, "Multisensor image fusion and enhancement in spectral total variation domain," IEEE Trans. Multimedia, 2017.
[4] A.S.A. Ghani and N.A.M. Isa, "Underwater image quality enhancement through composition of dual-intensity images and rayleigh-stretching," SpringerPlus, vol.3, no.1, p.757, 2014.
[5] L. Wang, H. Zhang, K. He, Y. Chang, X. Yang, and P.J. Atzberger, "Active contours driven by multi-feature gaussian distribution fitting energy with application to vessel segmentation," Plos One, vol.10, no.11, p.e0143105, 2015.
[6] K. Zhang, L. Zhang, K.-M. Lam, and D. Zhang, "A level set approach to image segmentation with intensity inhomogeneity," IEEE Trans. Cybern., vol.46, no.2, pp.546–557, 2016.
[7] A. Khadidos, V. Sanchez, and C.-T. Li, "Weighted level set evolution based on local edge features for medical image segmentation," IEEE Transactions on Image Processing A Publication of the IEEE Signal Processing Society, vol.26, no.4, pp.1979–1991, 2017.
[8] L.A. Vese and T.F. Chan, "A multiphase level set framework for image segmentation using the mumford and shah model," International Journal of Computer Vision, vol.50, no.3, pp.271–293, 2002.
[9] K. Zhang, H. Song, and L. Zhang, "Active contours driven by local image fitting energy," Pattern Recognition, vol.43, no.4, pp.1199–1206, 2010.
[10] K. Zhang, L. Zhang, K.M. Lam, and D. Zhang, "A level set approach

to image segmentation with intensity inhomogeneity," IEEE Trans. Cybern., vol.46, no.2, pp.546–557, 2016.
[11] C. Li, C.-Y. Kao, J.C. Gore, and Z. Ding, "Implicit active contours driven by local binary fitting energy," 2007 IEEE Conference on Computer Vision and Pattern Recognition, CVPR '07, pp.1–7, 2007.
[12] L. Wang, L. He, A. Mishra, and C. Li, "Active contours driven by local gaussian distribution fitting energy," Signal Processing, vol.89, no.12, pp.2435–2447, 2009.
[13] H. Yu, F. He, Y. Pan, and X. Chen, "An efficient similarity-based level set model for medical image segmentation," Journal of Advanced Mechanical Design, Systems, and Manufacturing, vol.10, no.8, pp.JAMDSM0100–JAMDSM0100, 2016.
[14] R.F. Wagner, S.W. Smith, J.M. Sandrik, and H. Lopez, "Statistics of speckle in ultrasound b-scans," IEEE Transactions on Sonics & Ultrasonics, vol.30, no.3, pp.156–163, 1983.
[15] T. Joel and R. Sivakumar, "Despeckling of ultrasound medical images: A survey," Journal of Image & Graphics, pp.161–165, 2013.
[16] L.R. Dice, "Measures of the amount of ecologic association between species," Ecology, vol.26, no.3, pp.297–302, 1945.

Hui Bi received the the M.Sc. degrees from Institute of Microelectronics of the Chinese Academy of Sciences (IMECAS), in 2010. Currently, she is working towards the Ph.D. degree at the Southeast University. Her research interests include statistical image processing, general visual object classification and video surveillance.

Yibo Jiang received the the M.Sc. and Ph.D. degrees from Institute of Microelectronics of the Chinese Academy of Sciences (IMECAS), in 2010 and 2013, respectively. Currently, he is an Assistant Professor at the Changzhou Institute of Technology. His research interests include medical imaging analysis and machine learning.

Hui Li received the Ph.D. degree in control theory and control engineering from the China University of Petroleum in 2013. Currently, he is an Assistant Professor at the Changzhou Institute of Technology. He current research interests include computational electromagnetics, image processing and numerical methods.

Xuan Sha received the B.S. degree in engineering mechanics in 2006 from Southeast University, Nanjing, China, and the M.S. degree in civil engineering in 2016 from Jiangsu University, Zhenjiang, China. Currently, she is working at the Chengxian College, Southeast University, Nanjing, China. Her research interests include image processing and its application in mechanics measurement, experimental photomechanics.

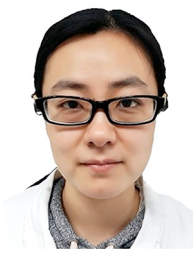

Yi Wang received her M.M. degree at Chongqing Medical University (Chongqing) (2009). Currently, She is she is working towards the Ph.D. degree at the Institute of Ultrasound Engineering in Medicine, Chongqing Medical University. Her research interest includes the therapy of high intensity focused ultrasound (HIFU), ultrasound contrast agent and biomedical applications.